Review

J. Astrophys. Astr. (2016) 37: 35
DOI: 10.1007/s12036-016-9413-x

Prospects of Measuring the Angular Power Spectrum of the Diffuse Galactic Synchrotron Emission with SKA1 Low

Sk. Saiyad Ali[1,*], Somnath Bharadwaj[2], Samir Choudhuri[2], Abhik Ghosh[3] & Nirupam Roy[2,4]

[1]*Department of Physics, Jadavpur University, Kolkata 700 032, India.*
[2]*Department of Physics and Centre for Theoretical Studies, Indian Institute of Technology Kharagpur, Kharagpur 721 302, India.*
[3]*Kapteyn Astronomical Institute, P.O. Box 800, 9700 AV Groningen, The Netherlands.*
[4]*Department of Physics, Indian Institute of Science, Bangalore 560 012, India.*
[*]*e-mail: saiyad@phys.jdvu.ac.in*

Received 14 May 2016; accepted 2 November 2016
ePublication: 28 November 2016

Abstract. The Diffuse Galactic Syncrotron Emission (DGSE) is the most important diffuse foreground component for future cosmological 21-cm observations. The DGSE is also an important probe of the cosmic ray electron and magnetic field distributions in the turbulent interstellar medium (ISM) of our galaxy. In this paper we briefly review the Tapered Gridded Estimator (TGE) which can be used to quantify the angular power spectrum C_ℓ of the sky signal directly from the visibilities measured in radio-interferometric observations. The salient features of the TGE are: (1) it deals with the gridded data which makes it computationally very fast, (2) it avoids a positive noise bias which normally arises from the system noise inherent to the visibility data, and (3) it allows us to taper the sky response and thereby suppresses the contribution from unsubtracted point sources in the outer parts and the side lobes of the antenna beam pattern. We also summarize earlier work where the TGE was used to measure the C_ℓ of the DGSE using 150 MHz GMRT data. Earlier measurements of C_ℓ are restricted to $\ell \leq \ell_{\rm max} \sim 10^3$ for the DGSE, the signal at the larger ℓ values is dominated by the residual point sources after source subtraction. The higher sensitivity of the upcoming SKA1 Low will allow the point sources to be subtracted to a fainter level than possible with existing telescopes. We predict that it will be possible to measure the C_ℓ of the DGSE to larger values of $\ell_{\rm max}$ with SKA1 Low. Our results show that it should be possible to achieve $\ell_{\rm max} \sim 10^4$ and $\sim 10^5$ with 2 minutes and 10 hours of observations respectively.

Key words. Methods: statistical, data analysis—techniques: interferometric—cosmology: diffuse radiation.

1. Introduction

Observations of the redshifted 21-cm radiation from the large scale distribution of neutral hydrogen (HI) have been perceived to be one of the most promising probes to study the high redshift Universe (Bharadwaj *et al.* 2001; also recent reviews by Morales & Wyithe 2010; Pritchard & Loeb 2012; Mellema *et al.* 2013). The principal challenge is to disentangle the cosmological 21-cm signal from the astrophysical foregrounds which are 4–5 orders of magnitude brighter (Ali *et al.* 2008; Bernardi *et al.* 2009; Ghosh *et al.* 2012). Several methods of foreground removal and foreground avoidance have been proposed in the literature for detecting the Epoch of Reionization (EoR) 21-cm signal (e.g. Chapman *et al.* 2014 and references therein).

Theoretical modelling and 150 MHz Giant Metrewave Radio Telescope (GMRT[1]; Swarup *et al.* 1991) observations show that extragalactic point sources are the most dominant foreground component at angular scales $\leq 4^\circ$ (Ali *et al.* 2008). These are also the angular scales relevant for telescopes like the LOw-Frequency ARray (LOFAR[2]; van Haarlem *et al.* 2013) and the upcoming Square Kilometre Array (SKA[3]; Koopmans *et al.* 2015). It is therefore clear that precise point source subtraction is essential for measuring the cosmological 21-cm signal. The residual data, after point source subtraction, is dominated by the diffuse synchrotron emission from our galaxy (Bernardi *et al.* 2009; Ghosh *et al.* 2012). There will also be a contribution from the residual point sources below the flux limit of the data. These two residuals can themselves be large enough to overwhelm the EoR 21-cm signal. Our present knowledge of the galactic diffuse metre wavelength radio emission is quite inadequate at arcminute and sub-arcminute angular scales. The mean spectral index of the synchrotron emission at high galactic latitude has been constrained to be $\alpha = 2.5 \pm 0.1$ in the 100–200 MHz range (Rogers & Bowman 2008). The angular power spectra of the diffuse galactic emission has been measured in only a few fields (Bernardi *et al.* 2009; Ghosh *et al.* 2012; Iacobelli *et al.* 2013). Both the spectral index and the angular power spectrum can vary significantly from field to field across different directions in the sky, and much remains to be done towards quantifying this. Further, the available measurements of the angular power spectrum of the diffuse galactic synchrotron radiation are restricted to $\ell \leq 1,300$, the signal at large ℓ being dominated by the residual point source contamination. The upcoming SKA is expected to achieve considerably greater sensitivity compared to the existing instruments, potentially leading to a better quantification and understanding of the different foregrounds. In particular, we can expect more accurate and deeper point source subtraction which should allow us to probe the angular power spectrum of the galactic synchrotron emission out to larger ℓ values (smaller angular scales) than previously achieved. In addition to being an important foreground component for the cosmological 21-cm signal, the study of the diffuse galactic synchrotron radiation is also important in its own right. The angular fluctuations of the synchrotron radiation are directly related to the fluctuations in the magnetic field and also the fluctuations in the electron density of the turbulent InterStellar Medium (ISM) of our galaxy (e.g. Waelkens *et al.* 2009; Lazarian & Pogosyan 2012; Iacobelli *et al.* 2013), a subject

[1] http://www.gmrt.ncra.tifr.res.in
[2] http://www.lofar.org/
[3] https://www.skatelescope.org

that is not very well understood at present. In this paper we review the methodology for measuring C_ℓ the angular power spectrum of the Diffuse Galactic Synchrotron Emission (hereafter, DGSE) using low frequency radio-interferometric observations, summarize some of the existing observational results and then discuss the prospects for the upcoming SKA.

In radio-interferometric observations, the quantity measured is the complex visibility. The measurement is done directly in Fourier space which makes interferometers ideal instruments to quantify the power spectrum of the sky signal. The visibility-based power spectrum estimators also have the added advantage that they avoid possible imaging artifacts due to the dirty beam, etc (Trott *et al.* 2011). A visibility-based estimator, namely the 'Bare Estimator', has been successfully employed to study the power spectrum of the HI in the ISM of several nearby galaxies (e.g. Begum *et al.* 2006; Dutta *et al.* 2009) and also applied to low frequency GMRT data to measure the angular power spectrum of the sky signal in the context of cosmological HI observations (Ali *et al.* 2008; Ghosh *et al.* 2011a). The bare estimator directly uses pairwise correlations of the measured visibilities to estimate C_ℓ, avoiding the self correlation that is responsible for a noise bias in the estimator. The bare estimator is very precise, but computationally very expensive for large data volumes, as the computation scales as the square of the number of visibilities (see Figures 6 and 12 in Choudhuri *et al.* 2014). The bare estimator has the added advantage that it does not pick up a noise bias which is an issue for many of the other estimators. For example, the image-based estimator (Seljak 1997) used by Bernardi *et al.* (2009) and Iacobelli *et al.* (2013) for C_ℓ and the visibility-based estimator (Liu & Tegmark 2012) for $P(k_\perp, k_\parallel)$ rely on modelling the noise properties of the data and subtracting out the expected noise bias. However, the actual noise in the observations could have baseline, frequency and time dependent variations which are very difficult to model, and there is always a possibility of residual noise bias contaminating the 21-cm signal. In a recent study, Paciga *et al.* (2011) have avoided the noise bias by cross-correlating the measured visibilities observed at different times. This, however, implies that only a part of the available data is actually being used to estimate the power spectrum.

In this paper, we highlight the Tapered Gridded Estimator (TGE) which is a novel estimator for measuring C_ℓ from the gridded visibility data. The TGE is computationally fast and does not pick up a noise bias contribution. It has the added feature of suppressing the contribution from the sidelobes and the outer regions of the antenna's field-of-view through a tapering of the sky response (Ghosh *et al.* 2011b). In section 2 of this paper, we briefly summarize the theoretical framework (Choudhuri *et al.* 2014, 2016a, b) for the TGE. In section 3, we review the earlier observational work (Ghosh *et al.* 2012) which has used GMRT data to quantify the angular power spectrum (C_ℓ) of the DGSE at 150 MHz. Finally, we predict the contribution of two major foregrounds namely the extra-galactic point sources and the DGSE, and make predictions for the prospects of measuring the DGSE using future 160 MHz observations with the upcoming SKA1 Low.

2. The tapered gridded estimator

In this section we briefly review the Tapered Gridded Estimator (TGE), the details of which are presented in Choudhuri *et al.* (2014). In any radio-interferometric

observations the measured visibilities $\mathcal{V}(\mathbf{U}, \nu)$ are a sum of two components namely the sky signal $\mathcal{S}(\mathbf{U}, \nu)$ and the system noise $\mathcal{N}(\mathbf{U}, \nu)$, i.e.

$$\mathcal{V}(\mathbf{U}, \nu) = \mathcal{S}(\mathbf{U}, \nu) + \mathcal{N}(\mathbf{U}, \nu)\,. \tag{1}$$

The entire analysis here is restricted to a particular frequency channel ν and we do not show this explicitly in the subsequent discussion.

We assume that the signal and the noise are both uncorrelated Gaussian random variables with zero mean. The measured visibilities record the Fourier transform of the product of the primary beam pattern $\mathcal{A}(\boldsymbol{\theta})$ and $\delta I(\boldsymbol{\theta})$ the angular fluctuation in the specific intensity of the sky signal. Here we use $\theta_{\rm FWHM}$ to denote the Full Width Half Maxima (FWHM) of $\mathcal{A}(\boldsymbol{\theta})$. The beam pattern $\mathcal{A}(\boldsymbol{\theta})$ is well modelled as a Gaussian $\mathcal{A}(\boldsymbol{\theta}) = \mathrm{e}^{-\theta^2/\theta_0^2}$ with $\theta_0 = 0.6 \times \theta_{\rm FWHM}$ in the central regions, the outer regions and the sidelobes however are typically not so well quantified and the beam pattern also varies with time as the antennas rotate to track a source on the sky. The TGE allows us to taper the sky response of the antenna elements and thereby suppresses the contribution coming from the outer part of the primary beam and the sidelobes. We implement the tapering by multiplying the field-of-view with a frequency-independent window function, $\mathcal{W}(\theta)$. Equivalently, in the Fourier domain we convolve the measured visibilities with $\tilde{w}(\mathbf{U})$, the Fourier transform of $\mathcal{W}(\theta)$. The convolved visibilities $\mathcal{V}_{\rm cg}$ are evaluated on a rectangular grid in uv space using

$$\mathcal{V}_{\rm cg} = \sum_i \tilde{w}(\mathbf{U}_g - \mathbf{U}_i)\, \mathcal{V}_i\,, \tag{2}$$

where $\mathbf{U}_{\rm g}$ refers to the different grid points and $\mathcal{V}_i$ refers to the visibility measured at a baseline $\mathbf{U}_i$. We have chosen a grid spacing $\Delta U = \sqrt{\ln 2}/(2\pi\theta_{\rm w})$ which corresponds to one fourth of the FWHM of $\tilde{w}(\mathbf{U})$ as an optimum value. Here, $\theta_{\rm w}$ is the tapering window which is used in the frequency-independent window function, $\mathcal{W}(\theta)$ (discussed later). For any fixed grid position $\mathbf{U}_{\rm g}$, we have restricted the contribution to baselines $\mathbf{U}_i$ within $|\mathbf{U}_{\rm g} - \mathbf{U}_i| \leq 6\Delta U$. The weight function $\tilde{w}(\mathbf{U}_{\rm g} - \mathbf{U}_i)$ falls considerably and we do not expect a significant contribution from the visibilities beyond this baseline. We note that the gridding process considerably reduces the data volume and the computation time required to estimate the power spectrum (Choudhuri *et al.* 2014). It may be noted that tapering the sky response is effective only if the window function $\tilde{w}(\mathbf{U}_{\rm g} - \mathbf{U}_i)$ in equation (2) is densely sampled by the baseline uv distribution. The GMRT has a patchy uv coverage and the tapering may not be very effective in this case. The width of the convolution window $\tilde{w}(\mathbf{U}_{\rm g} - \mathbf{U}_i)$ increases as the value of tapering factor f (discussed later) is reduced. The variation of the signal amplitude within the width of $\tilde{w}(\mathbf{U}_g - \mathbf{U}_i)$ becomes important at small baselines where it is reflected as an overestimate of the value of C_ℓ using TGE, though the excess is largely within the 1σ errors. This deviation is found to be reduced in a situation with a more uniform and denser baseline distribution like LOFAR (see Fig. 7 in Choudhuri *et al.* 2014 for details). The problem of the sparse uv coverage has been considerably reduced in an improved version of the TGE (Choudhuri *et al.* 2016c), we however do not discuss this here.

The convolved and gridded visibility data $\mathcal{V}_{\rm cg}$ gives an estimate of the Fourier transform of the product of the intensity fluctuations $\delta I(\boldsymbol{\theta})$ and a modified primary beam pattern $\mathcal{A}_{\mathcal{W}}(\boldsymbol{\theta}) = \mathcal{W}(\theta)\,\mathcal{A}(\boldsymbol{\theta})$. For the purpose of this paper we choose a

Gaussian window function $\mathcal{W}(\theta) = \mathrm{e}^{-\theta^2/\theta_{\mathrm{w}}^2}$ where we parametrize $\theta_{\mathrm{w}} = f\theta_0$ and refer to f as the tapering factor which should preferably have a value $f \leq 1$ so that the window function cuts off the sky response well before the first null of $\mathcal{A}(\boldsymbol{\theta})$. We can approximate the modified primary beam pattern as a Gaussian $\mathcal{A}_{\mathcal{W}}(\theta) = \mathrm{e}^{-\theta^2/\theta_1^2}$ with $\theta_1 = f(1+f^2)^{-1/2}\theta_0$. Figure 1 shows $\mathcal{A}(\boldsymbol{\theta})$ for the GMRT, and we have modelled this as a Bessel function corresponding to the diffraction pattern of a circular aperture of diameter 45 m. The figure also shows the modified primary beam pattern $\mathcal{A}_{\mathcal{W}}(\boldsymbol{\theta})$ for three different values $f = 3.0$, 1.0 and 0.7. For $f = 3.0$ we see that $\mathcal{A}_{\mathcal{W}}(\boldsymbol{\theta})$ is almost same as $\mathcal{A}(\boldsymbol{\theta})$ in the region within the first null, the difference however increases at the outer region of the primary beam beyond the first null. We see that the effective primary beam gets narrower as the value of f is reduced. The first side lobe of $\mathcal{A}_{\mathcal{W}}(\boldsymbol{\theta})$ is suppressed by a factor of $\approx 10^3$ (10^6) compared to $\mathcal{A}(\boldsymbol{\theta})$ at $|\boldsymbol{\theta}| = 4^\circ$ for $f = 1.0$ (0.7). We expect that for $f = 0.7$ the tapering will suppress by at least a factor of 10, the contribution from any residual point sources located beyond 2° from the phase center.

The correlation of the gridded visibilities $\langle \mathcal{V}_{\mathrm{cg}} \mathcal{V}_{\mathrm{cg}}^* \rangle$ provides a direct measurement of the angular power spectrum C_{ℓ_g}, the angular brackets here denote the ensemble average over many statistically independent realizations of the sky signal and the noise. In addition to the angular power spectrum C_ℓ, the correlation $\langle \mathcal{V}_{\mathrm{cg}} \mathcal{V}_{\mathrm{cg}}^* \rangle$ also picks up a contribution from the noise. This introduces a positive noise bias if we use $\langle \mathcal{V}_{\mathrm{cg}} \mathcal{V}_{\mathrm{cg}}^* \rangle$ to estimate C_ℓ. It is possible to eliminate this positive noise bias by subtracting out the self correlation of the visibilities (see section 5 of Choudhuri *et al.*

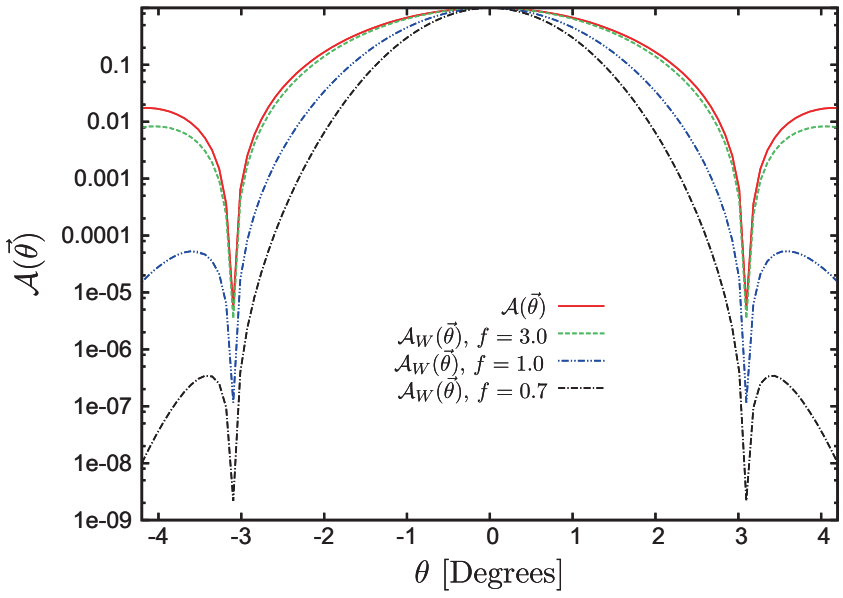

Figure 1. The GMRT 150 MHz primary beam $\mathcal{A}(\boldsymbol{\theta})$ which has been modelled as the square of a Bessel function. The effective primary beam $\mathcal{A}_{\mathcal{W}}(\boldsymbol{\theta})$, obtained after tapering the sky response for different values of f is also shown in the figure.

2014 for details). We use this to define the Tapered Gridded Estimator (TGE) at a grid point g as

$$\hat{E}_{\rm g} = \frac{(\mathcal{V}_{\rm cg}\mathcal{V}^*_{\rm cg} - \sum_i |\tilde{w}(\mathbf{U}_{\rm g} - \mathbf{U}_i)|^2 |\mathcal{V}_i|^2)}{(|K_{1\rm g}|^2 V_1 - K_{2\rm gg} V_0)}\,, \tag{3}$$

where the term $\sum_i |\tilde{w}(\mathbf{U}_{\rm g} - \mathbf{U}_i)|^2 |\mathcal{V}_i|^2$ has been introduced to cancel out the noise bias. The denominator of equation (3) is a normalization factor which converts the visibility correlation to the angular power spectrum, and here $V_0 = \frac{\pi\theta_0^2}{2}\left(\frac{\partial B}{\partial T}\right)^2$, $V_1 = \frac{\pi\theta_1^2}{2}\left(\frac{\partial B}{\partial T}\right)^2$, $K_{1\rm g} = \sum_i \tilde{w}(\mathbf{U}_g - \mathbf{U}_i)$, $K_{2\rm gg} = \sum_i |\tilde{w}(\mathbf{U}_{\rm g} - \mathbf{U}_i)|^2$, $B(T)$ is the Planck function and $\left(\frac{\partial B}{\partial T}\right)$ is the conversion factor from temperature to specific intensity.

The estimator $\hat{E}_{\rm g}$ defined here provides an unbiased estimate of $C_{\ell_{\rm g}}$ at the ℓ value $\ell_{\rm g} = 2\pi|\mathbf{U}_{\rm g}|$ corresponding to the grid point $\mathbf{U}_{\rm g}$, i.e.

$$\langle \hat{E}_{\rm g} \rangle = C_{\ell_{\rm g}}. \tag{4}$$

The $C_{\ell_{\rm g}}$ values estimated at different grid points are binned in logarithmic intervals of ℓ, and we consider the bin-averaged C_ℓ as a function of the bin-averaged angular multipole ℓ. We have implemented the TGE in our earlier paper (Choudhuri *et al.* 2014) where we have assumed a uniform and dense baseline uv coverage to calculate the normalization coefficient which relates visibility correlations to the estimated angular power spectrum C_ℓ. There we have found that this leads to an overestimate of C_ℓ of the sky signal (diffues galactic synchrotron emission) for instruments like the GMRT which have a sparse and patchy uv coverage. However, the overestimation is largely within the 1σ errors. This difference is found to be decreased in a situation with a more uniform and denser baseline distribution, like LOFAR. We have reduced this problem due to sparse and patchy uv sampling in an improved version of TGE (Choudhuri *et al.* 2016c) by calculating the normalization constant numerically using simulations.

The analysis presented in the paper has been restricted to observations at a single frequency wherein the relevant issue is to quantify the two angular fluctuations (e.g. C_ℓ) of the sky signal from the measured visibilities. This, however, is inadequate for the three dimensional redshifted HI 21-cm signal where it is necessary to also simultaneously quantify the fluctuations along the frequency direction. It may be noted that in a very recent work (Choudhuri *et al.* 2016c), the TGE has been further generalized to quantify the three dimensional power spectrum of the 21-cm brightness temperature fluctuations $P(k_\perp, k_\parallel)$, we however do not discuss this here.

The TGE has three key features:

(a) It works directly with the measured visibilities after *gridding* the data in the uv plane. This significantly reduces the data volume and thereby reduces the computation required to estimate the power spectrum. This is relevant in the context of the current and the next generation radio-interferometers which are expected to produce large volumes of visibility data in observations spanning many frequency channels and large observing times.

(b) It is difficult to image and subtract point sources from the outer parts and the sidelobes of the telescope's field-of-view. The residual point sources in the outer regions of the field-of-view pose a problem for estimating the power spectrum of

the diffuse radiation like the galactic synchrotron radiation or the cosmological 21-cm radiation. The TGE enables us to estimate the power spectrum with a *tapered* sky response. This suppresses the contribution from the outer regions and the sidelobes of the telescope's beam pattern.

(c) The system noise inherent to the observations typically introduces a positive noise bias in the estimated power spectrum. The TGE is devised in such a way that it internally computes the noise bias and subtracts this out to provide an $unbiased$ estimate of the power spectrum of the sky signal.

3. Results and conclusion

In this section, we briefly summarize and discuss the results originally presented in Ghosh *et al.* (2012). Here the TGE was applied to the visibility data from GMRT 150 MHz observations in four different fields referred to as Fields I, II, III and IV respectively. The discussion here is restricted to Field I which is the only field where it was possible to detect the angular power spectrum of the diffuse galactic synchrotron radiation. The residual point source contamination was too high for the galactic synchrotron radiation to be detected in the three other fields.

Field I was centered at sky position with RA = 05 h 30 m 00 s and Dec = $+60^\circ\ 00'\ 00''$ with a frequency bandwidth of 8 MHz centered at 150 MHz, however only a frequency width of 3.75 MHz was used for the final analysis. A continuum image of the field was first used to identify point sources to a limiting flux of 10 mJy. This corresponds to $\sim$7 times the off-source RMSs noise of 1.3 mJy/beam obtained in the continuum image. The point sources were subtracted from the visibility data, and the residual visibilities were used for the subsequent analysis.

The TGE was applied to the visibility data to estimate the angular power spectrum C_ℓ both before and after the point sources were subtracted. The analysis used the value $f = 0.8$ for the tapering parameter. The results are shown in Figure 2 which has been reproduced from Ghosh *et al.* (2012). It is clearly visible that subtraction of the point sources causes the sky signal to fall considerably at all angular multipoles. The C_ℓ for the residual data after point source subtraction clearly shows different behaviour in two different ranges of l. At low angular multipoles ($\ell \leq 800$), which correspond to angular scales larger than $10'$, we find a steep power law behavior which is typical of the galactic synchrotron emission observed at higher frequencies and larger angular scales (e.g. Bennett *et al.* 2003). The angular power spectrum flattens out for $\ell > 800$, and we find that it remains nearly flat out to $\ell \approx 8,000$ which corresponds to angular scales of $\sim 1'$. The nearly flat region arises from the residual point sources which have a flux below the threshold for source identification, and hence have not been subtracted from the data. There is also a contribution from the residuals arising from errors in modelling the brighter point sources. The residual point source contribution dominates C_ℓ at small angular scales where we are unable to make out the galactic synchrotron radiation.

It is clear from this analysis that C_ℓ, after point source subtraction, is dominated by the diffuse galactic synchrotron emission at $\ell \leq 800$ which corresponds to $\sim 10'$. We have used a weighted least square to fit a power law model

$$C_\ell^M = A \times \left(\frac{1000}{\ell}\right)^\beta \tag{5}$$

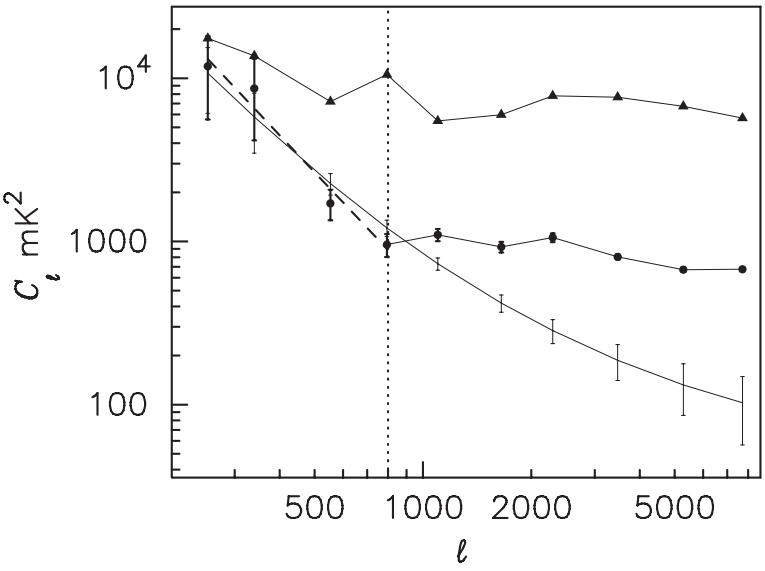

Figure 2. This shows the measured C_ℓ before (triangle), and after (circle) point source subtraction. The 1σ error-bars are shown only for the residual data after subtracting the sources above $S_c = 10$ mJy. The residual artifacts after point source subtraction have a peak flux $\sim$20 mJy. The dashed line shows the best fit power-law for $\ell \leq 800$. The thin solid line (bottom curve) with 1 - σ error-bars shows the model prediction of Ali *et al.* (2008) assuming that all point sources above $S_c = 20$ mJy have been identified and removed from the data. This figure is reproduced from Ghosh *et al.* (2012).

to the measured C_ℓ for $\ell \leq 800$. We find the best fit values $A = 513 \pm 41\,\mathrm{mK}^2$ and $\beta = 2.34 \pm 0.28$ for which C_ℓ^M is also shown in Fig. 2. Our findings are consistent with those of Bernardi *et al.* (2009) who have analysed 150 MHz WSRT observations. They have subtracted out point sources above 15 mJy, and used the resulting image to estimate the angular power spectrum C_ℓ which they find is well described by a power law for $\ell \leq 900$. There has also been considerable work on modelling the galactic synchrotron radiation at higher frequencies relevant for the cosmic microwave background radiation (CMBR) (tens of GHz). These works predict a power law behaviour $C_\ell \propto \ell^{-\beta}$ where β has values in the range 2.4 to 3 down to $\ell = 900$ (Tegmark & Efstathiou 1996; Tegmark *et al.* 2000). Giardino *et al.* (2002) have analysed the 2.4 GHz Parkes radio continuum survey of total intensity of the southern galactic plane where they found a slope $\beta = 2.37 \pm 0.21$ across the range $40 \leq \ell \leq 250$. Our slope, measured at smaller angular scales, is consistent with these findings.

As mentioned earlier, the DGSE is the most important diffuse foreground for observations of the cosmological 21-cm signal. The study of the DGSE is also important in its own right as it allows us to probe the cosmic ray electron and magnetic filed distributions in the turbulent ISM of our galaxy. We now discuss the prospects of measuring the angular power spectrum C_ℓ of the DGSE using 160 MHz observations with the upcoming SKA1 Low. Present measurement of the C_ℓ of the DGSE at 150 MHz are restricted to $\ell \leq \ell_{\mathrm{max}} = 900$, the signal at larger angular multipoles

is dominated by the residual point sources after point source subtraction. It is anticipated that future observations with SKA1 Low will allow the point sources to be identified and subtracted down to a lower limiting flux S_c than possible in the earlier observations described here. This should, in turn, allow us to measure the C_ℓ of the DGSE out to a larger value of $\ell_{\rm max}$ thereby allowing us to probe the structure of the turbulent ISM at smaller angular scales than those possible in earlier observations.

Table 6 of Prandoni & Seymour (2015) shows that one expects to achieve a $5\,\sigma$ noise level of $\sim 6\,\mu$Jy/beam in ~ 8 h of observation in a single field with SKA1 Low. We use this to estimate the limiting flux S_c for future SKA1 Low observations, assuming that all sources above the $5\,\sigma$ noise level can be identified and subtracted. We further assume that the $5\,\sigma$ noise level falls inversely as the square-root of the observing time, and therefore the limiting flux can lowered by having longer observations. We use this to model the angular power spectrum C_ℓ of the sky signal as the value of S_c is lowered (Fig. 3). Our prediction for C_ℓ incorporates the two most dominant components, namely the point sources and the DGSE. The model prediction for the DGSE is based on the angular power spectrum C_ℓ^M (equation (5)) measured in 150 MHz GMRT observation (Ghosh *et al.* 2012). Point sources make two distinct contributions to the angular power spectrum, the first being the Poisson fluctuation due to the discrete nature of the sources and the second arising from the clustering of the sources. The point source contribution is predicted using the differential source count measured at 150 MHz (Ghosh *et al.* 2012) and a power law index of 1.1 for the angular two-point correlation $\omega(\theta)$ at 1.4 GHz (Cress *et al.* 1996). For the purpose of the predictions, the DGSE contribution has been extrapolated from 150 MHz to 160 MHz using a mean spectral index of 2.52 from Rogers & Bowman (2008).

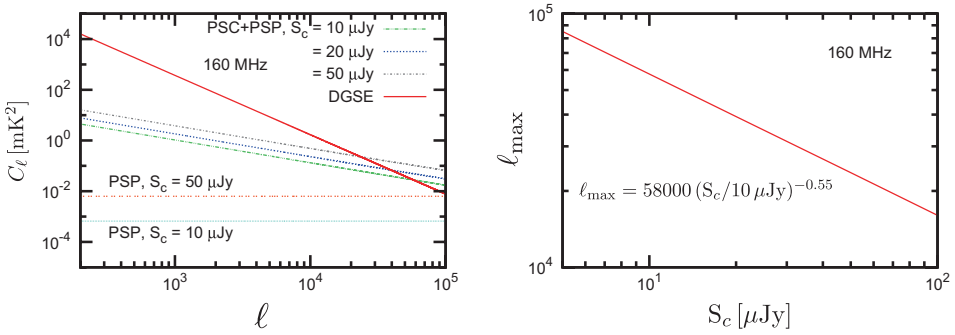

Figure 3. *Left panel*: Considering 160 MHz SKA1 Low observations, this shows the model predictions for the angular power spectrum C_ℓ of the two major radio-sky components namely the DGSE and the point sources. The point source contribution itself is a combination of two components, the Point Source Clustering (PSC) and the Point Source Poisson (PSP) contributions respectively. The results for the point sources are shown for the different values of the limiting flux S_c indicated in the figure. It is assumed that all the discrete sources brighter than S_c have been identified in the image and subtracted from the visibility data. *Right panel*: This shows the maximum value of the angular multipole ($\ell_{\rm max}$) below which ($\ell \le \ell_{\rm max}$) we expect to measure C_ℓ for the DGSE, the signal is expected to be dominated by the residual point sources at $\ell > \ell_{\rm max}$. The figure shows how the value of $\ell_{\rm max}$ varies with S_c. The value of $\ell_{\rm max}$ is obtained by equating the total point source contribution (PSC+PSP) to the contribution from the DGSE (see the left panel). We find that the relation between $\ell_{\rm max}$ and S_c is well fitted by the power law shown in the figure.

Similarly, we have extrapolated the point source contribution to 160 MHz using an average spectral index of 2.7 (Jackson 2005; Randall *et al.* 2012). The framework for modelling the expected C_ℓ has been presented in detail in Ali *et al.* (2008).

The left panel of Fig. 3 shows the total point source contribution to C_ℓ predicted for three different values of the limiting flux $S_c = 10\,\mu$Jy, $20\,\mu$Jy and $50\,\mu$Jy respectively. The two horizontal dotted lines show just the Poisson contribution for $S_c = 10\,\mu$Jy and $50\,\mu$Jy respectively. The Poisson contribution falls very rapidly as S_c is lowered, and we see that the Poisson component is sub-dominant to the clustered component at all values of ℓ for the S_c values which we have considered here. The DGSE contribution shown in Fig. 3 does not change with S_c. We see that the DGSE is the most dominant component at $\ell \leq \ell_{\rm max} = 2 \times 10^4$ and $\ell \leq \ell_{\rm max} = 5 \times 10^4$ for $S_c = 50\ \mu$ Jy and 10 μJy respectively. We clearly see that future observations with the upcoming SKA1 Low are expected to probe the DGSE at angular multipoles which are much larger than those where we currently have measurements.

The right panel of Fig. 3 shows how the value of $\ell_{\rm max}$ changes as the value of S_c is varied. The largest angular multipole where we currently have measurements of the DGSE is around $\ell_{\rm max} \sim 10^3$. We see that it is possible to achieve $\ell_{\rm max} \sim 10^4$, i.e. and order of magnitude increase in $\ell_{\rm max}$, with $S_c = 100\,\mu$Jy which one expects to achieve in approximately 2 minutes of observation with SKA1 Low. We find that the relation between $\ell_{\rm max}$ and S_c is well fitted by the power law $\ell_{\rm max} = 58000\,(\mathrm{S}_c/10\,\mu\mathrm{Jy})^{-0.55}$. This power law implies that we expect $\ell_{\rm max}$ to increase as $t^{0.275}$ as the observing time t is increased, and we can expect to achieve $\ell_{\rm max} \sim 10^5$ in approximately 10 h of observation.

In conclusion, we note that present measurement of the angular power spectrum C_ℓ of the diffuse galactic synchrotron emission are restricted to $\ell \leq l_{\rm max} \sim 10^3$. Future observations with the upcoming SKA1 Low are expected to allow us to probe this at much larger multipoles. Our predictions show that one expects to achieve $\ell_{\rm max}$ in the range 10^4 to 10^5 using observations that span a few minutes to tens of hours in duration.

Acknowledgements

We thank the anonymous referee for useful comments and suggestions. SC would like to acknowledge the University Grant Commission (UGC), India for providing financial support through Senior Research Fellowship. SSA would like to acknowledge CTS, IIT Kharagpur for the use of its facilities. SSA would also like to thank the authorities of IUCAA, Pune, India for providing the Visiting Associateship programme.

References

Ali, S. S., Bharadwaj, S., Chengalur, J. N. 2008, *MNRAS*, **385**, 2166.
Begum, A., Chengalur, J. N., Bhardwaj, S. 2006, *MNRAS*, **372**, L33.
Bennett, C. L. *et al.* 2003, *ApJS*, **148**, 97.
Bernardi, G, de Bruyn, A. G., Brentjens, M. A. *et al.* 2009, *A&A*, **500**, 965.
Bharadwaj, S., Nath, B. B., Sethi, S. K. 2001, *JApA*, **22**, 21.
Chapman, E., Zaroubi, S., Abdalla, F. *et al.* 2014, arXiv:1408.4695.

Choudhuri, S., Bharadwaj, S., Ghosh, A., Ali, S. S. 2014, *MNRAS*, **445**, 4351.
Choudhuri, S., Bharadwaj, S., Roy, N., Ghosh, A., Ali, S. S. 2016a, *MNRAS*, **459**, 151.
Choudhuri, S., Roy, N., Bharadwaj, S., Ali, S. S., Ghosh, A., Dutta, P. 2016b, submitted to *MNRAS*.
Choudhuri, S., Bharadwaj, S., Chaterjee, S., Ali, S. S., Roy, N., Ghosh, A., Ali, S. S. 2016c, submitted to *MNRAS*.
Cress, C. M., Helfand, D. J., Becker, R. H., Gregg, M. D., White, R. L. 1996, *ApJ*, **473**, 7.
Dutta, P., Begum, A., Bharadwaj, S., Chengalur, J. N. 2009, *MNRAS*, **398**, 887.
Ghosh, A., Bharadwaj, S., Ali, S. S., Chengalur, J. N. 2011a, *MNRAS*, **411**, 2426.
Ghosh, A., Bharadwaj, S., Ali, S. S., Chengalur, J. N. 2011b, *MNRAS*, **418**, 2584.
Ghosh, A. *et al.* 2012, *MNRAS*, **426**, 3295.
Giardino, G., Banday, A. J., G'orski, K. M., Bennett, K., Jonas, J. L., Tauber, J. 2002, *A&A*, **387**, 82.
Iacobelli, M., Haverkorn, M., Orrú, E. *et al.* 2013, *A&A*, **558**, A72.
Jackson, C. 2005, *PASA*, **22**, 36.
Koopmans, L., Pritchard, J., Mellema, G. *et al.* 2015, *Advancing Astrophysics with the Square Kilometre Array (AASKA14),* 1.
Lazarian, A., Pogosyan, D. 2012, *Ap.J*, **747**, 5.
Liu, A., Tegmark, M. 2012, *MNRAS*, **419**, 3491.
Mellema, G. *et al.* 2013, *Experimental Astronomy*, **36**, 235.
Morales, M. F., Wyithe, J. S. B. 2010, *ARAA*, **48**, 127.
Paciga, G. *et al.* 2011, *MNRAS*, **413**, 1174.
Prandoni, I., Seymour, N. 2015, *Advancing Astrophysics with the Square Kilometre Array (AASKA14)* p. 67.
Pritchard, J. R., Loeb, A. 2012, *Rep. Prog. Phys.*, **75(8)**, 086901.
Randall, K. E., Hopkins, A. M., Norris, R. P. *et al.* 2012, *MNRAS*, **421**, 1644.
Rogers, A. E. E., Bowman, J. D. 2008, *ApJ*, **136**, 641.
Seljak, U. 1997, *ApJ*, **482**, 6.
Swarup, G., Ananthakrishnan, S., Kapahi, V. K., Rao, A. P., Subrahmanya, C. R., Kulkarni, V. K. 1991, *Curr. Sci.*, **60**, 95.
Tegmark, M., Efstathiou, G. 1996, *MNRAS*, **281**, 1297.
Tegmark, M., Eisenstein, D. J., Hu, W, de Oliveira-Costa, A. 2000, *ApJ*, **530**, 133.
Trott, C. M., Wayth, R. B., Macquart, J.-P. R., Tingay, S. J. 2011, *Ap.J*, **731**, 81.
van Haarlem, M. P., Wise, M. W., Gunst, A. W. *et al.* 2013, *A&A*, **556**, A2.
Waelkens, A. H., Schekochihin, A. A., Enßlin, T. A. 2009, *MNRAS*, **398**, 1970.